TEMPORAL OCCURRENCE AND FORECASTING
OF LANDSLIDES IN THE EUROPEAN COMMUNITY
CONTRACT EPOCH N°90 0025 (DTEE)

Final report. Oct.1993

Part I: Methodology (Reviews) for the Temporal Study of Landslides

MODELLING OF DEBRIS FLOW

H. M. BLIJENBERG[1]

1 Department of Physical Geography, University of Utrecht, Netherlands

INTRODUCTION

Debris flows are defined as a rapid mass movement of granular solids, water and air, moving as a viscous flow (Varnes, 1978). Their movement type, gravity flow, differs from landslides, in which a more or less rigid mass slides along a distint shear surface, as well as from streamflow, where the material is transported by the shear forces caused by streamflow rather than by gravity. They occur in many mountainous and semiarid regions all over the world. Figures 1 and 2 show some examples of debris flows.

The effects of debris flows can be catastrophic when they occur in densely populated areas. In Japan alone about 90 people a year die as a result of debris flows. Well-known is the catastrophic debris flow that resulted from the sudden melt of a glacier caused by the eruption of the Nevado del Ruiz in Colombia in 1988. The flow buried the village of Armero and over 30.000 people died. A more recent example is the debris flow that occurred in september 1992 in the department Drôme in south-east France. As a result of intense rainfall during several days a debris flow was initiated which followed the course of the Ouvèze river and ruined a part of the historic village Vaison-la-Romaine, causing several casualties.

As the dimensions of debris flows may vary over many orders of magnitude, Innes (1983) proposed a scale classification for debris flows based on the volume of the deposits: microscale ($<1m^3$), smallscale ($1\text{-}10^3m^3$), mediumscale ($10^3\text{-}10^5m^3$) and largescale ($>10^5m^3$) debris flows. Other classification systems have been proposed. For example, a distinction can be made between valley-confined and (unconfined) hillslope debris flows (Brunsden, 1979).

Within the EPOCH project 'The Temporal Analysis of Debris Flows in an Alpine Environment' attention is mainly focused on smallscale hillslope debris flows in a part of the southern French Alps. These flows usually show a typical morphology: a long, small, ribbonlike channel bordered by lateral levees which meet downslope in a lobate or tongue-shaped terminal deposit, as can be seen in figure 2. Hovius (1990) describes typical debris flow source areas in the Bachelard valley as spoon- or funnel-shaped concave parts of slopes (Fig.3). Downslope they are confined by an outcrop of resistant bedrock through which the source areas are drained by a narrow channel. Slope angles within typical source areas are between 33° and 38°. On the channel floors coarse debris has accumulated, transported by rockfall. The slopes bordering the channels consist of either solid bedrock or more or less fine-grained regolith. Vegetation is largely absent in source areas, except for some herbes and grasses.

Final aim of the project is to forecast initiation and frequency of debris flows on the basis of morphologic and hydrologic characteristics of debris flow source areas and of precipitation characteristics. Figure 4 presents a highly simplified diagram representing the research 'framework'. It combines two models, a stability model and a hydrologic model, to forecast debris flow initiation.

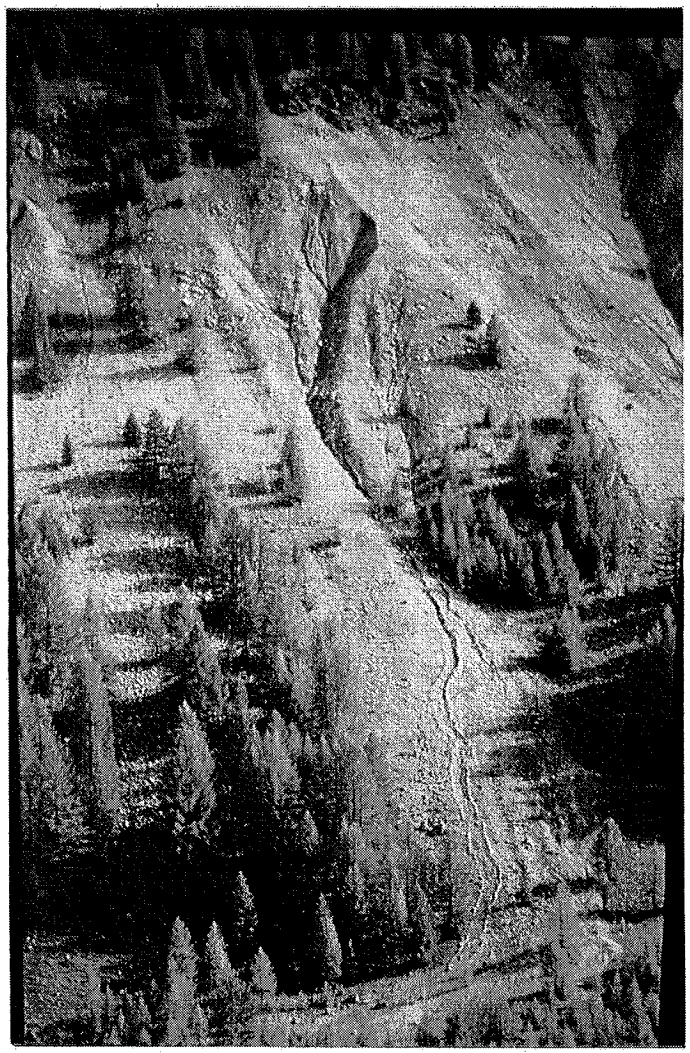

Figure 1: A typical debris flow on the west-facing slope of the Tête du Clot des Pastres.

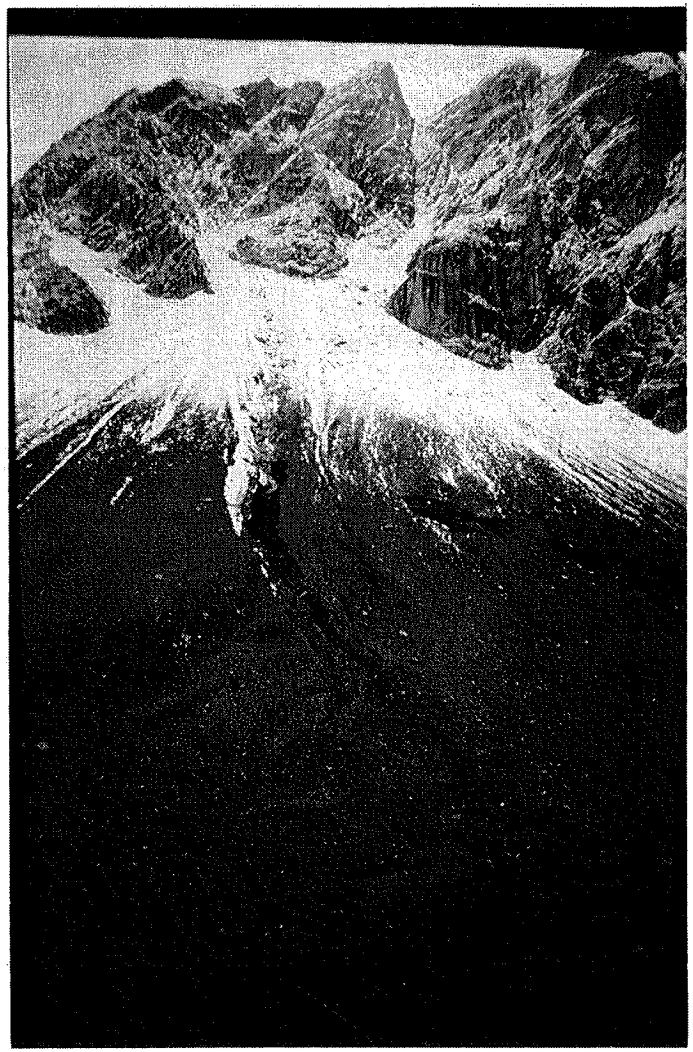

Figure 2: A debris flow showing the typical morphology: a channel bordered by lateral levees, and a terminal lobe-shaped deposit.

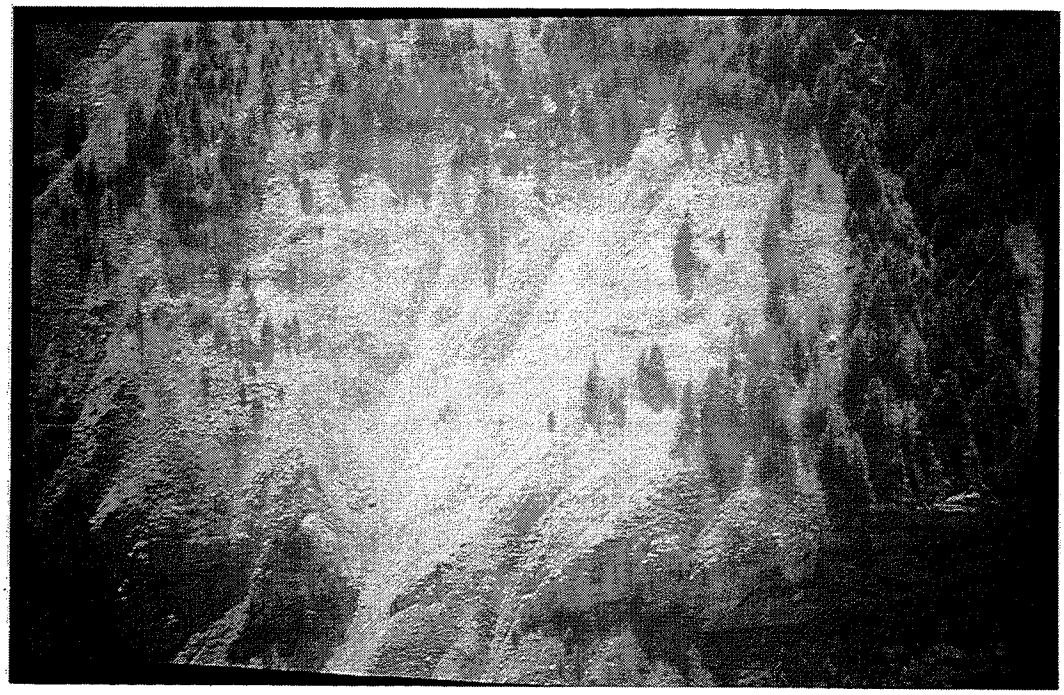

Figure 3: A typical debris flow source area: Pra Bouréou South.

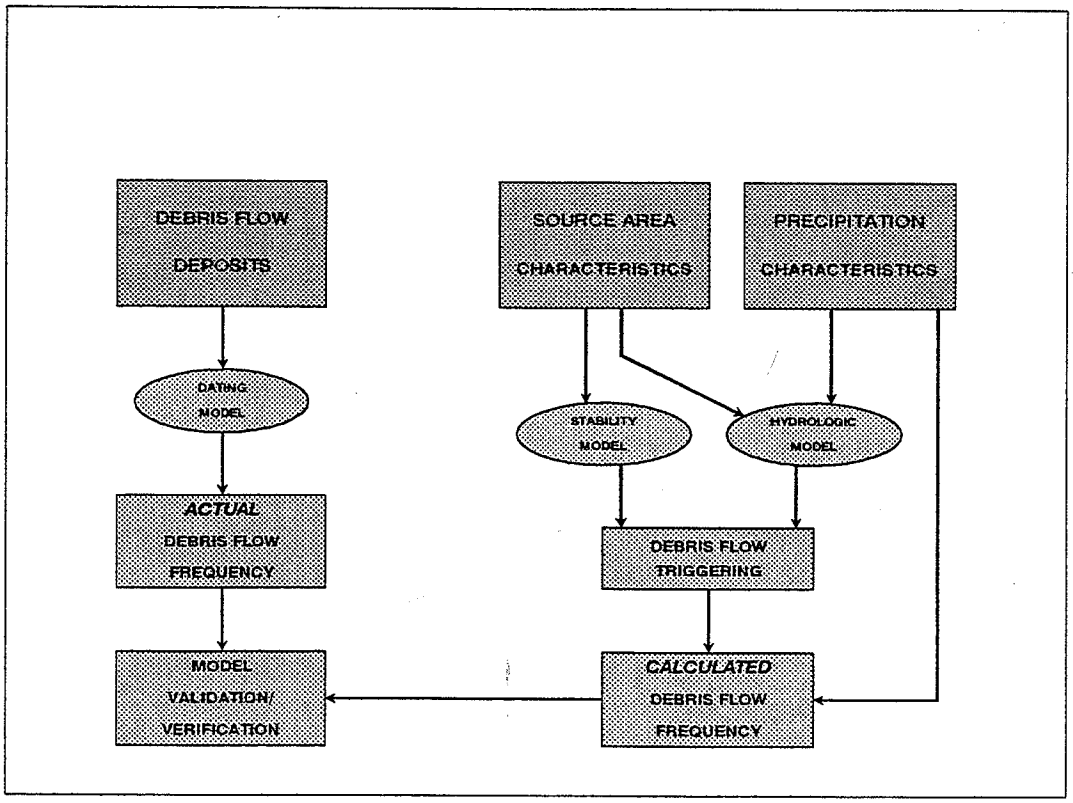

Figure 4: Schematic representation of the study: initiation and frequency of debris flows.

DEBRIS FLOW INITIATION

Prerequisites for the occurrence of debris flows are steep slopes, high pore pressures, available debris and a loss of consistency of the material after initiation of movement. Debris flows can be initiated in many different ways. The best known initiation mechanisms are the transformation of landslides into debris flow by dilatancy or liquefaction during movement (e.g. Johnson, 1970; Johnson & Rodine, 1984), and the spontaneous initiation of debris flows by dilatancy (Takahashi 1978, 1980, 1981). Dilatancy is the increase of bulk volume which causes the incorporation of additional water. Liquefaction is the loss of strength caused by a (sudden) increase of pore pressure. Other possible mechanisms include spontaneous liquefaction, damming of water behind debris dams (Costa, 1984) and the 'firehose effect' caused by the impact of a high-speed stream of water (Johnson & Rodine, 1984).

External forces can trigger the movement: vibrations caused by earthquakes, passing debris flows or volcanic eruptions, and impact or loading forces by snow avalanches or mass movements (Bovis & Dagg, 1987). Usually however an increase of pore pressures caused by a supply of water to the material provides the trigger for initiation of movement. Water can be supplied by rainfall, snowmelt or a combination of both. Less frequent water supplies include drainage of crater lakes, rapid snow and ice melt during volcanic eruptions, glacial outburst floods and stream diversions.

Johnson (1970) and Johnson & Rodine (1984) give examples of surficial landslides transforming into debris flows. Therefore, their stability criterion for initiation of a debris flow is the same as the stability criterion of a landslide sliding parallel to the surface. The stability is given by the infinite slope model (Fig.5):

$$F = [c' + (\gamma - m\gamma_w)\, z \cos^2\beta \tan\varphi'] / \gamma z \sin\beta \cos\beta \qquad 1$$

where

F	= stability factor (-)
c'	= effective cohesion (Pa)
m	= relative groundwater level (-)
γ	= (dry) bulk weight of debris ($N \cdot m^{-3}$)
γ_w	= unit weight of water ($N \cdot m^{-3}$)
z	= depth of failure surface (m)
β	= slope angle of (failure) surface (°)
φ'	= effective angle of internal friction (°)

When $F = 1$ the mass is at the point of failure. As soon as $F < 1$ failure will occur and the mass will start sliding. The transformation is caused by either dilatancy or liquefaction during movement.

On short time scales groundwater level is the only variable factor in equation (1). A rise of groundwater level causes an increase of pore pressure in the debris mass. Pore pressure increase may also be caused by external forces like earthquakes or rockfall.

According to Takahashi (1978, 1980, 1981) an accumulation of debris lying on a gully floor may spontaneously turn into a debris flow. This may happen by dilatancy as soon as a water film of a certain thickness h_0 appears at the surface of a saturated body of debris. Figure 6 gives three different situations distinguished by Takahashi. The force equilibrium model used by Takahashi is also based on an infinite slope situation. Mathematically, the shear stress at depth z is given by:

$$\tau = g \sin\beta \, [c* (\sigma - \rho)z + \rho (z + h_0)] \qquad 2$$

and the shear resistance by:

$$\tau_L = g \cos\beta \, [c* (\sigma - \rho)z] \tan\varphi \qquad 3$$

where

τ = shear stress (Pa)
τ_L = shear resistance (Pa)
g = gravitational acceleration (9.81 $m \cdot s^{-2}$)
σ = solids density ($kg \cdot m^{-3}$)
ρ = liquid density ($kg \cdot m^{-3}$)
$c*$ = volumetric content of solids of static debris (-)
z = depth (m)
h_0 = depth of waterflow above surface (m)
β = slope angle (°)
φ = angle of internal friction of debris (°)

Figure 6 a shows the situation of a non-stationary bed, when shear stress increases faster with depth than shear resistance:

$$d\tau/dz > d\tau_L/dz \qquad 4$$

In this situation the whole bed of debris will start to move. The combination of equations (2) and (3) yields the critical slope angle:

$$\tan\beta \geq [c* (\sigma - \rho) / c* (\sigma - \rho) + \rho] \tan\varphi \qquad 5$$

If $h_0 = 0$ or the body of debris is not fully saturated, failure may still occur. However, in this situation there is not enough water available for the debris to dilate and lose consistency, so a landslide is formed rather than a debris flow.

In figure 6 b and c the shear resistance of the debris increases faster with

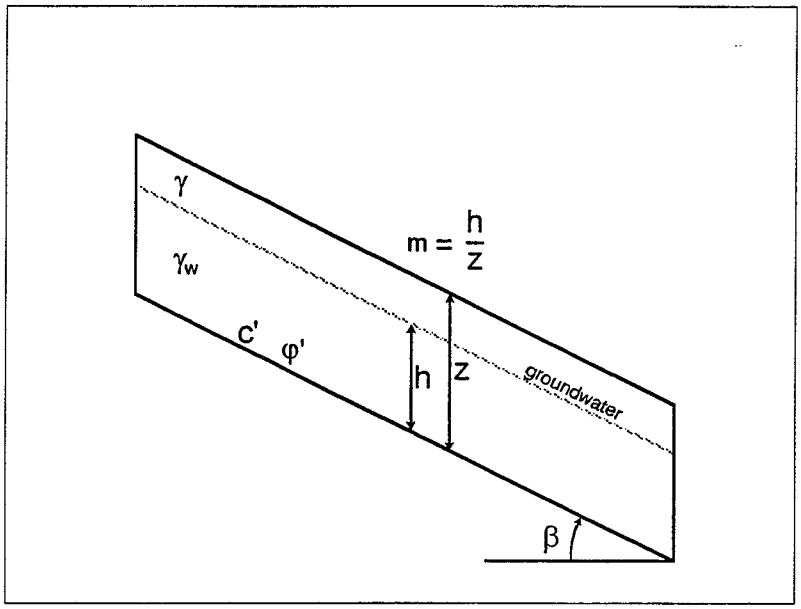

Figure 5: Forces on a soil wedge on an 'infinite' slope.

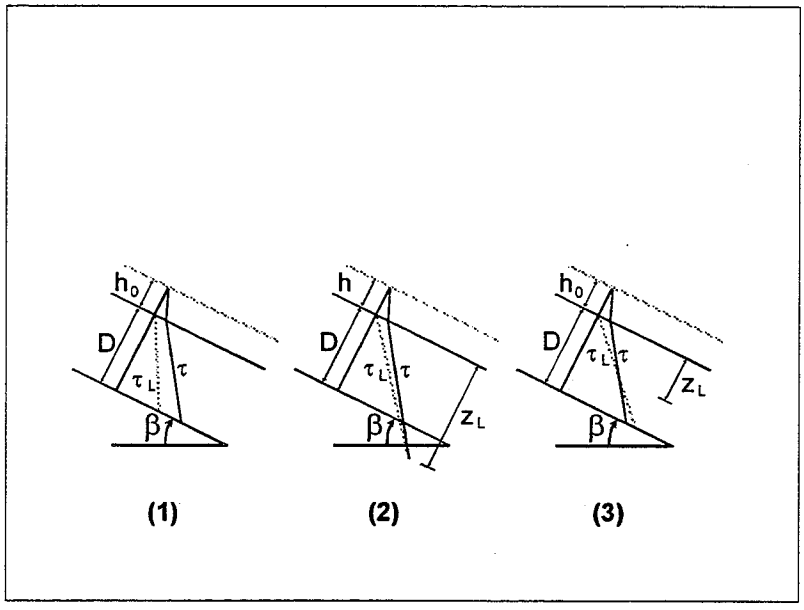

Figure 6: Characteristic shear stress distributions in a debris layer according to Takahashi (1978, 1980, 1981).

depth than the shear stress:

$$d\tau/dz < d\tau_L/dz \qquad 6$$

For this situation failure can only occur if $h_0 > 0$. At a certain depth z_L the shear stress and the shear resistance are equal and up to this depth failure will occur. In situation two, where z_L is deeper than the base of the debris accumulation, the limit of moving and stable material is formed by the gully floor. The third situation gives the situation, in which not all of the debris mass will move. This is the (quasi-)stationary bed situation. Takahashi gives an additional boundary condition for this case:

$$z_L \geq d \qquad 7$$

where
d = characteristic grain diameter (m)

If $z_L < d$, no debris flow situation can take place, only transport by streamflow. The following equation gives the condition that must be fulfilled for the occurrence of a debris flow:

$$c_* (\sigma - \rho) / [c_* (\sigma - \rho) + \rho (1 + h_0/d)] \tan\varphi \leq \tan\beta < [c^* (\sigma - \rho)/c^* (\sigma - \rho) + \rho] \tan\varphi \qquad 8$$

Another boundary condition is given by Takahashi:

$$z_L \geq k h_0 \qquad 9$$

where
k = dimensionless coefficient (-)

This boundary condition is introduced to exclude situations in which there is too much water to have the debris uniformly dispersed throughout the depth of flow. Usually k is about 1. Combination of equations (8) and (9) gives the critical slope angle for the occurrence of debris flows:

$$\tan\beta = [c_* (\sigma - \rho) / c_* (\sigma - \rho) + \rho (1 + 1/k)] \tan\varphi \qquad 10$$

For realistic values ($c_* = 0.7$; $\sigma = 2600$ kg·m^{-3}; $\rho = 1000$ kg·m^{-3}; $k = 0.75$; $\tan\varphi = 0.8$) debris flows may occur on slopes of 14.5°-22.9°.

Bovis & Dagg (1988) also used the model developed by Takahashi (1978, 1980, 1981). They emphasized the importance of the hydraulic conductivity of the debris bed. The conductivity is not a constant, but changes in time as a result of

selective removal of finer material by streamflow action. As mean pore size is increased, the conductivity will increase as well. Equation (11) is the empirical relationship given by Bovis & Dagg (1988) to calculate the hydraulic conductivity:

$K = u \phi / s^b$

where

K	= hydraulic conductivity ($m \cdot s^{-1}$)
u	= mean flow velocity in debris ($m \cdot s^{-1}$)
ϕ	= porosity (-)
s	= hydraulic gradient (-)
b	= coefficient (-): 1.0 for laminar and 2.0 for fully turbulent flow

The increase of conductivity causes an increase of the stability of the debris mass as the discharge needed to reach a critical groundwater level in the mass is increased. The increase in hydraulic conductivity can be many orders of magnitude. Bovis & Dagg (1988) give an example in which conductivity may have increased by a factor 10^3. Besides the large increase of conductivity, the angle of internal friction may slightly increase as fine material is washed out. According to Bovis & Dagg (1988) the increase may be about 2° from 37° for hillslope colluvium to 39° for coarse channel deposits.

Debris flow research done by students in the eighties had shown that none of the above-mentioned initiation mechanisms was realistic enough for the study area. On gully floors coarse, cohesionless debris was present, whereas on the side-slopes much fine-grained material was present. A hypothesis was formulated by Postma (1988) and Hovius (1990) that during high-intensity rainstorms overland flow occurred which would entrain much of the fine material. The muddy flow has a high density compared to water and has a different viscosity. This mud would run over and enter into the pores of the coarse debris on the gully floor and may destabilize this coarse debris. The mixed material will then continue to move as a debris flow. Figure 7 gives the flow chart of this hypothesis. The hypothesis differs from Takahashi's (1978) model on several points:

Takahashi assumes the presence of all grain size fractions in the gully, whereas in this hypothesis a separation exists between coarse debris on the gully floors and the relatively fine-grained material on the side-slopes.

The hydraulic conductivity of the coarse, cohesionless debris in the gully is much higher than that of the debris assumed by Takahashi.

Instead of water, the fluid entering the pores of the coarse debris is a mixture of water and fine debris with higher density and higher viscosity than water.

Fluid is not only supplied from upstream through the gully, as assumed by Takahashi, but also from the side slopes of the gully.

Postma (1988) has given a mathematical formulation of the hypothesis. She assumed that instability of the debris mass will occur as soon as it is fully saturated with the muddy fluid (Fig.8), i.e. when the discharge of fluid into the coarse debris equals the maximum dicharge that can flow through the debris. For laminar flow conditions Bernouilli's law can be used to calculate the discharge q_v through the coarse debris:

$$\Delta p / \rho g + \Delta (u^2) /2g + \Delta z = Rq_v \qquad \textbf{12}$$

where

Δp	$= p_2 - p_1$	with p1, p2 the fluid stress at points 1 and 2 (Pa)
$\Delta(u^2)$	$= u^2_2 - u^2_1$	with u_1, u_2 the flow velocity at points 1 and 2 ($m \cdot s_1$)
Δz	$= z_2 - z_1$	with z_1, z_2 the ... at points 1 and 2 (m)
ρ	= fluid density ($kg \cdot m^3$)	
g	= gravitational acceleration (9.81 $m \cdot s^{-2}$)	
R	= viscous resistance ($s \cdot m^{-1}$)	
q_v	= discharge of fluid through coarse debris ($m^2 \cdot s^{-1}$)	

The viscous resistance can be obtained from the following equation:

$$R = \Delta x/DK \qquad \textbf{13}$$

where

Δx	= distance (m)
D	= depth of coarse debris layer (m)
K	= (hydraulic) conductivity of saturated debris ($m \cdot s^{-1}$)

As can be derived from figure 8, fluid stress and flow velocity are equal in the points 1 and 2, which gives:

$$q_v = DK\sin\beta \qquad \textbf{14}$$

where

β	= slope angle (°)

From equation (14) it follows that the critical supply of muddy fluid depends on slope angle, debris depth and debris hydraulic conductivity. It is difficult to determine the hydraulic conductivity K of coarse debris, and even more difficult for fluids consisting of a mixture of water and fine-grained material.

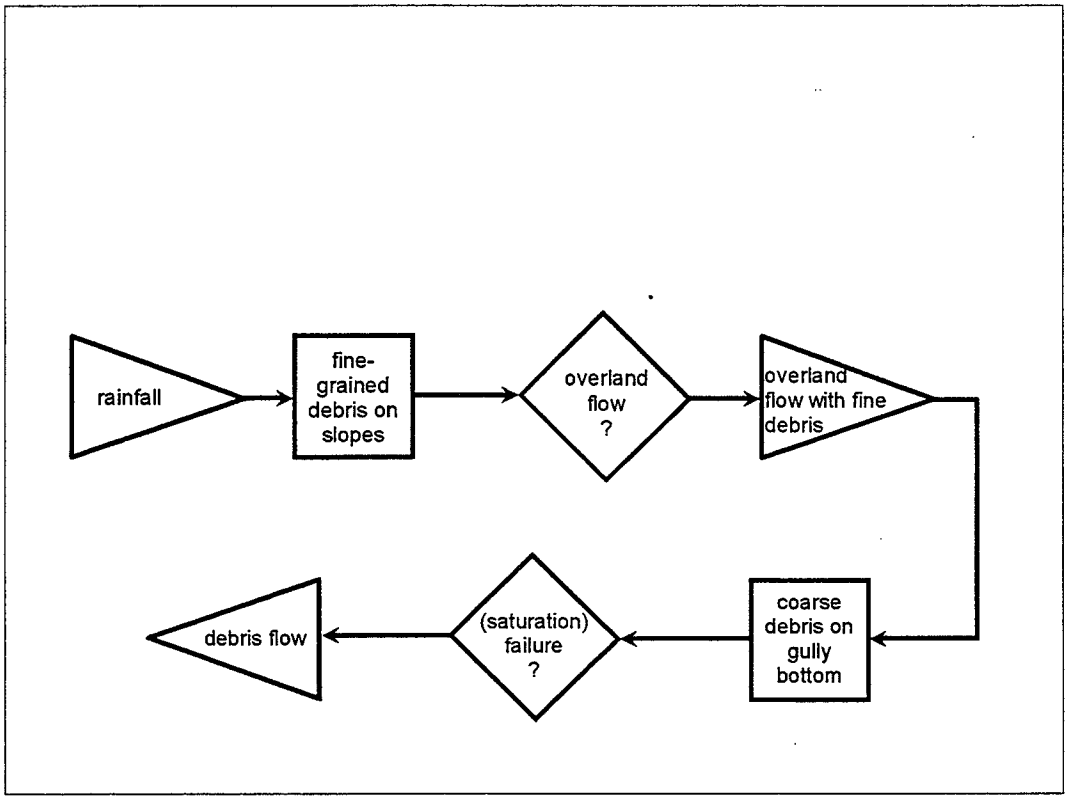

Figure 7: Flow chart of debris flow initiation according to Postma (1988).

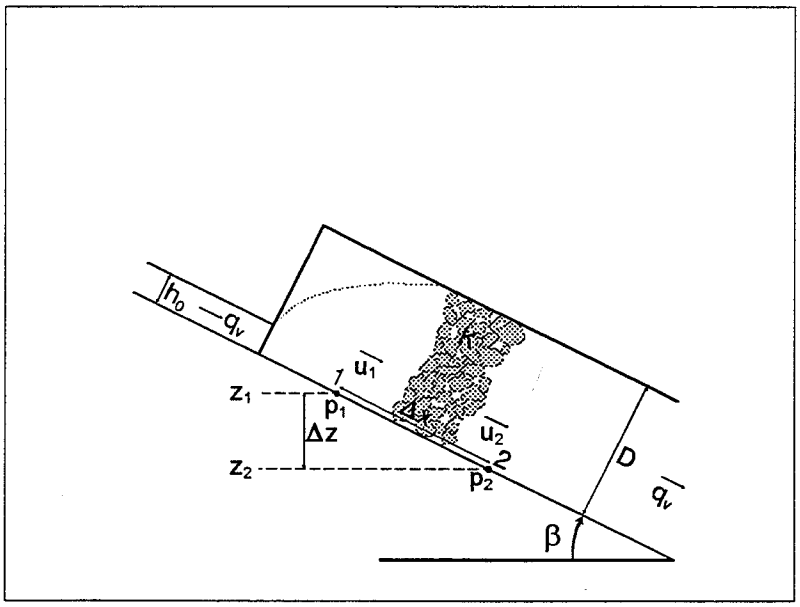

Figure 8: Discharge through a saturated debris layer.

WATER AS THE KEY VARIABLE FOR DEBRIS FLOW INITIATION

The most important factor causing instability on short time scales in all the models presented is the amount of water available. Rainfall is the most important water supply in the study area. For debris flows and shallow landslides triggered by rainfall Caine (1980) found a curve of minimum rainfall intensity from a literature survey:

$$i_r = 14.82\ D^{-0.39} \qquad \textbf{15}$$

where
i_r = rainfall intensity (mm/hr)
D = rainfall duration (hr)

Debris flows are unlikely when $i_r < 14.82 \cdot D^{-0.39}$. A similar curve has been constructed by Innes (1983) for debris flows, using total rainfall instead of rainfall intensity:

$$I_r = 4.94\ D^{0.50} \qquad \textbf{16}$$

where
I_r = total rainfall in period (mm)

In the study area high-intensity short-duration rainstorms trigger most debris flows; according to eye-witness observations 5-10 minutes of 50-100 mm/hr rainfall intensity are sufficient for debris flow initiation (van Asch & van Steijn, 1991). Long-duration low-intensity rainfall and snowmelt hardly produce debris flows. The high intensities needed and the very quick response make it likely that infiltration excess overland flow is responsable for the initiation of debris flows, rather than saturation overland flow or subsurface flow. The overland flow is mainly produced from bedrock slopes and slopes covered with fine-grained regolith.

Therefore, modelling the amount of water available is the same as modelling the amount of water that does not infiltrate the ground, and tracing this water through the debris flow source areas.

When rain falls on a surface, two situations may occur. First, the ground may be impervious, leaving all the rain water at the surface. Second, the ground may be permeable and a part of or all of the rain will infiltrate. The first case can be found in those areas where solid bedrock outcrops. The other situation is usually found in areas where a regolith is present, but sometimes this may occur as well on solid bedrock if it is permeable like some sandstones or limestones.

To model the amount of water available for overland flow in debris flow source areas for any rainfall event a distinction was made between parts with solid bedrock, with fine-grained regolith, and parts with coarse debris at the surface. It is assumed that solid bedrock is impervious, coarse debris is extremely permeable relative to rainfall intensities occurring in the area, and fine-grained regolith has in-

between characteristics. Modelling the amount of water available for overland flow using this assumptions is very simple for the bedrock and the coarse debris, leaving only modelling the infiltration of the fine-grained regolith.

During rainstorms infiltration excess (Hortonian) overland flow may occur on the regolith slopes. Rainfall intensity, rainfall duration and the infiltration capacity of the regolith determine whether or not overland flow will occur. The infiltration capacity of the regolith is not constant, but it generally decreases with time until a constant value is reached, the steady state infiltration capacity. Cumulative infiltration is given by:

$$I = Kt + St^{1/2} \qquad \textbf{17}$$

where

I = cumulative infiltration (L)
t = time (T)
K = steady state infiltration capacity (LT^{-1})
S = sorptivity ($LT^{-½}$)

The steady state infiltration capacity usually is a little less than the saturated hydraulic conductivity K_{sat}. This is caused by the enclosure of air bubbles in the pores during infiltration. In practice, however, K_{sat} is often used instead of K. This gives the widely used Philips' (1957) mass infiltration equation for ponded infiltration (Fig.9):

$$I\ K_{sat}\ t + St^{1/2} \qquad \textbf{18}$$

Which after differentiation gives:

$$i = K_{sat} + 1/2\ St^{-1/2} \qquad \textbf{19}$$

where i = infiltration capacity (LT^{-1})

Sorptivity is the dominant factor during the first phase of infiltration (Dunin, 1976). It represents the absorption of water by a dry soil. This absorption depends on soil texture and structure and on the initial water content of the soil. Green & Ampt (1911) have developed an analytical solution for infiltration (Fig.10) based on the decrease of the hydraulic head with time during infiltration. The following assumptions have been used:

The initial water content, τ_i, is constant throughout the non-infiltrated zone.

Throughout the infiltrated zone the volume fraction of water, τ_t, is uniform and constant with time.

The change of τ_i to τ_t at the wetting front takes place in a layer of negligible thickness.

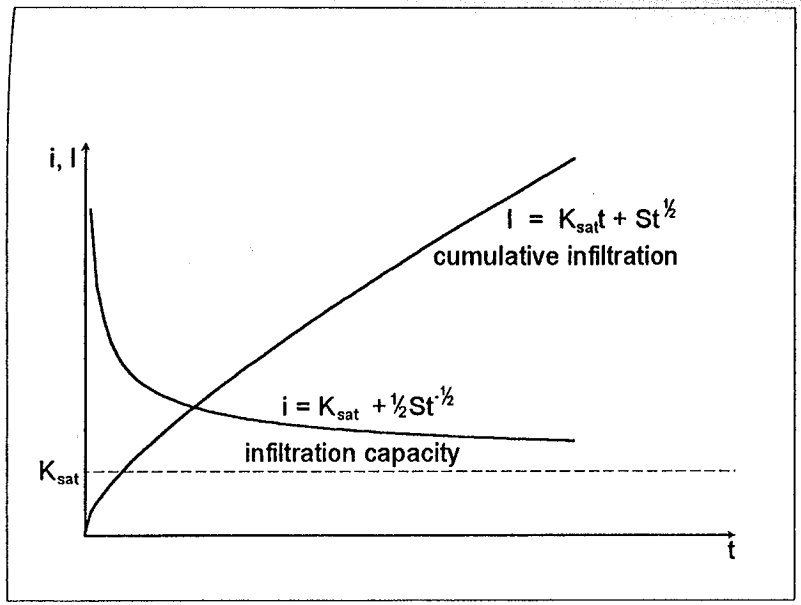

Figure 9: Infiltration curves according to Philips (1957).

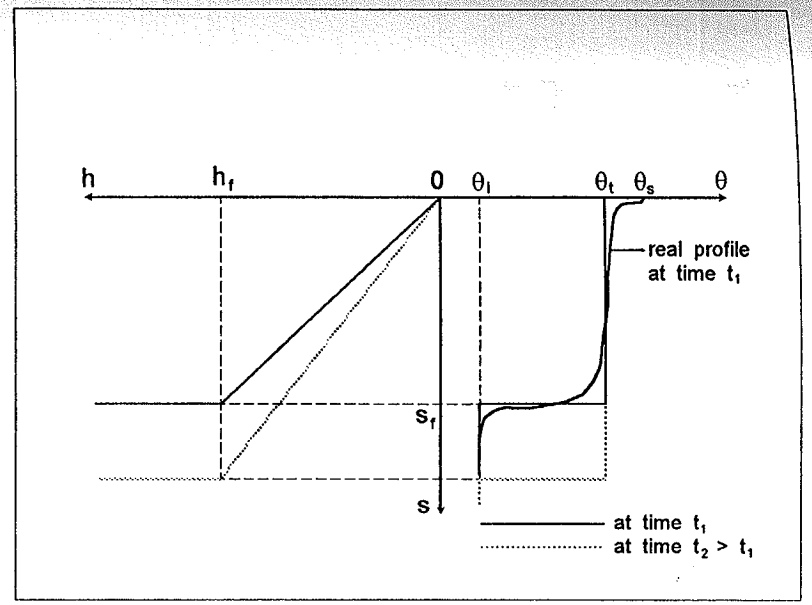

Figure 10: Soil water distribution during (ponded) infiltration according to Green & Ampt (1911).

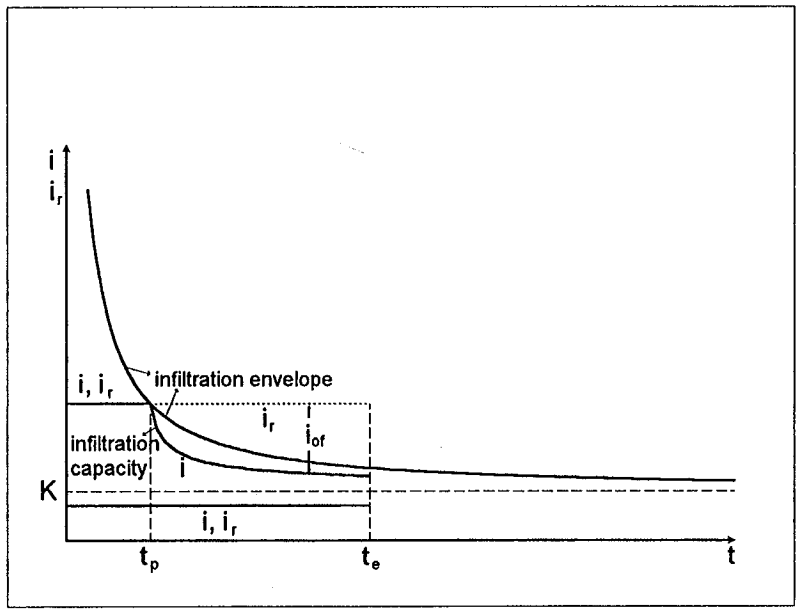

Figure 11: The infiltration capacity during a rainfall event and its relation to the infiltration envelope.

- The pressure head at the wetting front, h_f, has a constant value, independent of the position of the wetting front, s_f.

- The water layer at the soil surface has a negligible thickness: $h_0 = 0$ at $s = 0$.

These assumptions are realistic for infiltration into coarse-textured soils with low initial water content, as can be found in the regolith slopes in debris flow source areas in the study area.

From the second assumption it follows that throughout the transmission zone the hydraulic conductivity, K_t, is constant. The flux density, q, is also constant throughout the transmission zone at any moment. Using the last three assumptions, Darcy's law can be rewritten:

$$i = q = - K [\partial H/\partial s] = -K [\partial h/\partial s + \partial z/\partial s] = -K_t [h_f/s_f - 1] \quad \textbf{20}$$

where
i = infiltration capacity of the soil ($m \cdot s^{-1}$)
q = flux density ($m \cdot s^{-1}$)
K_t = hydraulic conductivity of transmission zone ($m \cdot s^{-1}$)
H = hydraulic head (m)
h = pressure head (m)
z = gravitational head (m)
s = distance (m)

Cumulative infiltration can be derived from the continuity equation:

$$I = \int_{s=0}^{\infty} (\theta_t - \theta_i)\, ds = (\theta_t - \theta_i)\, s_f \quad \textbf{21}$$

and:

$$i = dI/dt = (\theta_t - \theta_i)\, ds_f/dt \quad \textbf{22}$$

Combining with equation (20) gives:

$$K_t(1 - h_f/s_f) = (\theta_t - \theta_i)\, ds_f/d_t \quad \textbf{23}$$

As sorptivity is dominant in the early stages of infiltration, gravity can be neglected:

$$- K_t\, (h_f/s_f) = (\theta_t - \theta_i)\, ds_f/dt \quad \textbf{24}$$

After integration, with the condition $s_f = 0$ at $t = 0$, the following equation is obtained:

$$sf = [-2K_t h_f / \theta_t - \theta_i]^{1/2} t^{1/2} \qquad \textbf{25}$$

which can be read as $s_f/\sqrt{t}$ = constant, i.e. the depth of the wetting front increases proportional with the square root of time. Entering the solution into equation (21) gives:

$$I = [-2 K_t h_f (\theta_t - \theta_i)]^{1/2} t^{1/2} \qquad \textbf{26}$$

And from equation (18) it follows that, when gravity is neglected:

$$S = [-2K_t h_f (\theta_t - \theta_i)]^{1/2} \qquad 27$$

which gives a physical meaning to the sorptivity parameter.

When rainfall intensity is less than or equal to the steady state infiltration capacity, the infiltration rate will equal the rainfall intensity. When the rainfall intensity is higher than the steady state infiltration capacity, a slightly different situation occurs. The infiltration capacity decreases with time until at time t_p it equals the rainfall intensity (Fig.11). At this moment ponding will start, and the time t_p is called the time-to-ponding. For $t > t_p$ the infiltration rate will be determined by the monotonically decreasing infiltration capacity. As this is less than the rainfall intensity, infiltration-excess overland flow will occur. The place of ponding point t_p of the infiltration curve depends on rainfall intensity. t_p increases with decreasing rainfall intensity and is infinite for a rainfall intensity equal to the steady state infiltration capacity. The curve obtained by connecting the ponding points of infiltration rate curves for different rainfall intensities is called the infiltration envelope. The infiltration envelope approaches K for $t \rightarrow \infty$. The equation for an infiltration envelope is given by Smith & Parlange (1978):

$$_0\int^{tp} i_r dt = A/K \ln (i_r/i_r - K) \qquad \textbf{28}$$

where

$_0\int^{tp} i_r dt$ = total amount of rainfall until ponding (L)

i_r = rainfall intensity (LT^{-1})

A = $\frac{1}{2}S^2$ (L^2T^{-1})

The total amount of runoff can be calculated by summation of the difference between rainfall intensity and infiltration capacity from t_p until the time when rainfall stops, t_e, as long as rainfall intensity is higher than the infiltration capacity:

$$I_{0f} = {}_{tp}\int^{te} (i_r - i)\, dt = {}_{tp}\int^{te} i_r\, dt + \underset{tp}{\overset{te}{[S\,(t - t_0)^{1/2} + K(t-t_0)]}} \quad \text{for } i_r \geq i \qquad \textbf{29}$$

where
I_{of} = total amount of overland flow (L)

and:

$$t0 = tp - [S^2 / 4(i_r-K)^2 \qquad \textbf{30}$$

is the virtual starttime (t = 0) of the infiltration curve of equation (17).

The water that can not infiltrate into the regolith will start to flow downslope over the steep slopes in the debris flow source areas. Several types of runoff models will be used to model the runoff in debris flow source areas.

A very simple model is the exponential storage model, which can be seen as a very simple tank model. In this model the discharge Q from a catchment is proportional to the amount of water present in the catchment:

$$Q = \alpha V = - (dV/dt) \qquad \textbf{31}$$

where
V = total amount of water in catchment (L^3)
α = catchment constant (T^{-1})

The change of the amount of water can be written as:

$$dV/dt = A(i_r - i) - Q = A\,(i_r - i) - \alpha V \qquad \textbf{32}$$

where
A = surface of source area (L^2)
i_r-i = the rainfall surplus (L)

The total amount of water in the catchment at time t is obtained by integration:

$$V = V + \int [A(i_r - i) - Q = A\,(i_r - i) - \alpha V]dt = Ve^{-\alpha dt} + \int A(i_r-i)dt \qquad \textbf{33}$$

and the discharge by taking the value of V from equation (33) in equation (31).

The discharge of the monitored catchment has been modelled using the GIS PC-RASTER. One of the modules of this GIS-package is the program WATERSHED, that can be used to calculate catchment discharge (van Deursen & Kwadijk, 1990). Every time step the water present in a pixel is transported one pixel downslope. The downslope direction is determined as the steepest slope downwards to one of eight neighbouring pixels using a digital terrain model of the catchment. The transport over one pixel for each time step implies that the time steps have to be chosen to conform to the real displacement of the water over one pixel distance in one time step. This type of calculation does not make a differentiation between (subsurface flow,) sheetflow and channelflow possible. Values of the infiltration parameters K and S in each pixel of the catchment were drawn randomly from a known frequency distribution of these parameters that had been obtained from the field measurements. The frequency distributions of the randomly drawn values agree with those of the field data.

Difficult parameters in the water flow modelling are fluid density and viscosity. These parameters depend on the amount of sediment entrained in the water and appear in many flow equations. They also determine the character of the flow, i.e. whether the flow is laminar or turbulent. The sediment content of the flow usually is not constant during a rainstorm, but may be very variable, as found by Olyphant et al. (1991).

RUN OUT MODELLING OF DEBRIS FLOWS

The mobility of the debris flows and therefore the run out distance depends basically on two factors:
- The viscous behaviour of the flow.
- The strength characteristics in terms of c and φ

It can be proved that, despite the high velocities of the flows, there is rate dependent strength within these high mobile masses. This means that flow adopts its velocity to the slope angles along the flow path. This can be expressed by the simple physical law:

$$\tau/\tau_0 = 1/F \; a \log v + b \qquad 34$$

where

τ	= shear stress
τ_0	= mobile shear strength
1/F	= inverse of the Safety Factor (F)
v	= velocity of the flow
a, b	= constants, related to the mobility of landslides

Equation (34) and also other viscous laws show that the velocity is linear or exponential correlated to the shear stress τ which itself is related to the sine of slope times the weight component of the debris mass. There is no permanent acceleration or deceleration because of the excessive shear stress over shear strength as is the case with the large catastrophic slope failures.

A good illustration of the viscous strength behaviour of these debris flows can be given with the data given by Suwa and Okuda (1985). The velocity of different debris flows could be measured at 16 points along the same flow path over a horizontal distance of 2300 m in the Kamikamihori valley in Japan.

The velocity of the debris flows can be described by energy lines showing the movement of the point of gravity in relation to the energy line of frictional loss along the flow path. The difference in height between these two lines gives the velocity of movement at that point which is equal to $v_2/2g$. (Sassa, 1988) (Fig.12). If there exists no viscous rate dependent strength in the material the friction line is dependent on the internal mobile friction of the material which can be constant during movement (straight line a in figure 12), or there may be an increase of the friction due to the loss of water (line b); or first a decrease of friction due to generation of heat and high pore pressures and then an increase in strength due to pore pressure dissipation (line c). There are more alternative patterns which depend on the mechanism of the flow (or slide). All these patterns however show accelerations and decelerations which are not directly related to the underlying slope angle of the flow path.
In flows with a viscous strength however, the friction line tan φ_a follows the same angle as the gravity line tan (Fig.12 line d.) In other words the resistance increases with velocity to a level where $\tan\varphi_a = \tan\theta$. The angle of the friction line therefore follows the angle of the gravity line.

In figure 13 a profile is given of the flow path of the Kamikamihori debris flows. The measured velocities along the flow path are multiplied by a factor $v^2/2g$ (= m; Fig.12) and plotted as vertical length at the observation points above the gravity line (which is the slope profile of the track, Fig.13). It can be seen that the friction line follows the gravity line. The velocities varies between 0.5 and 5 m/sec hence $v^2/2g$ between 0.012 and 1.25 m which is not observable on the graph. If no viscous drag component was present in these flows, the friction may have a more or less constant value which is given by the line a in figure 12. In that case velocities would have been 10 to 100 times higher than the measured velocities.

The question remains whether the relation between 1/F and the velocity is linear or exponential. In the latter case velocities can become extremely catastrophic at higher excess shear stresses and the viscous drag component does not play a role any more. Figure 14 shows 1/F -velocity relationships obtained from debris flows in the French Alps in the basin of Barcelonnette. The data show no clear trend towards an exponential relationship but the data are very scattered due to changes in water content and hence viscosity along the flow path.

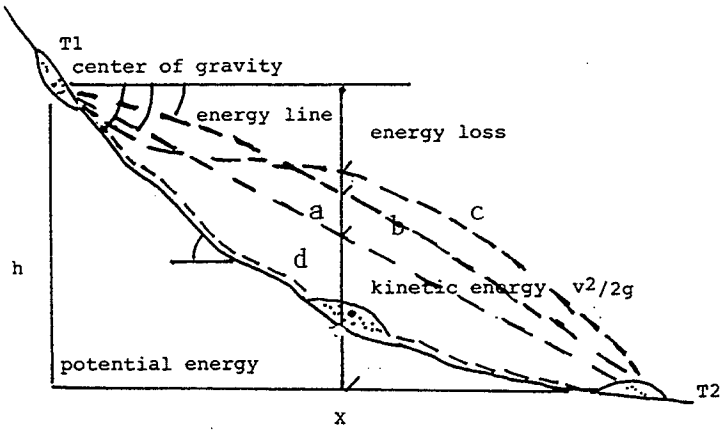

Figure 12: Friction lines and energy loss during run out of different types of landslides.

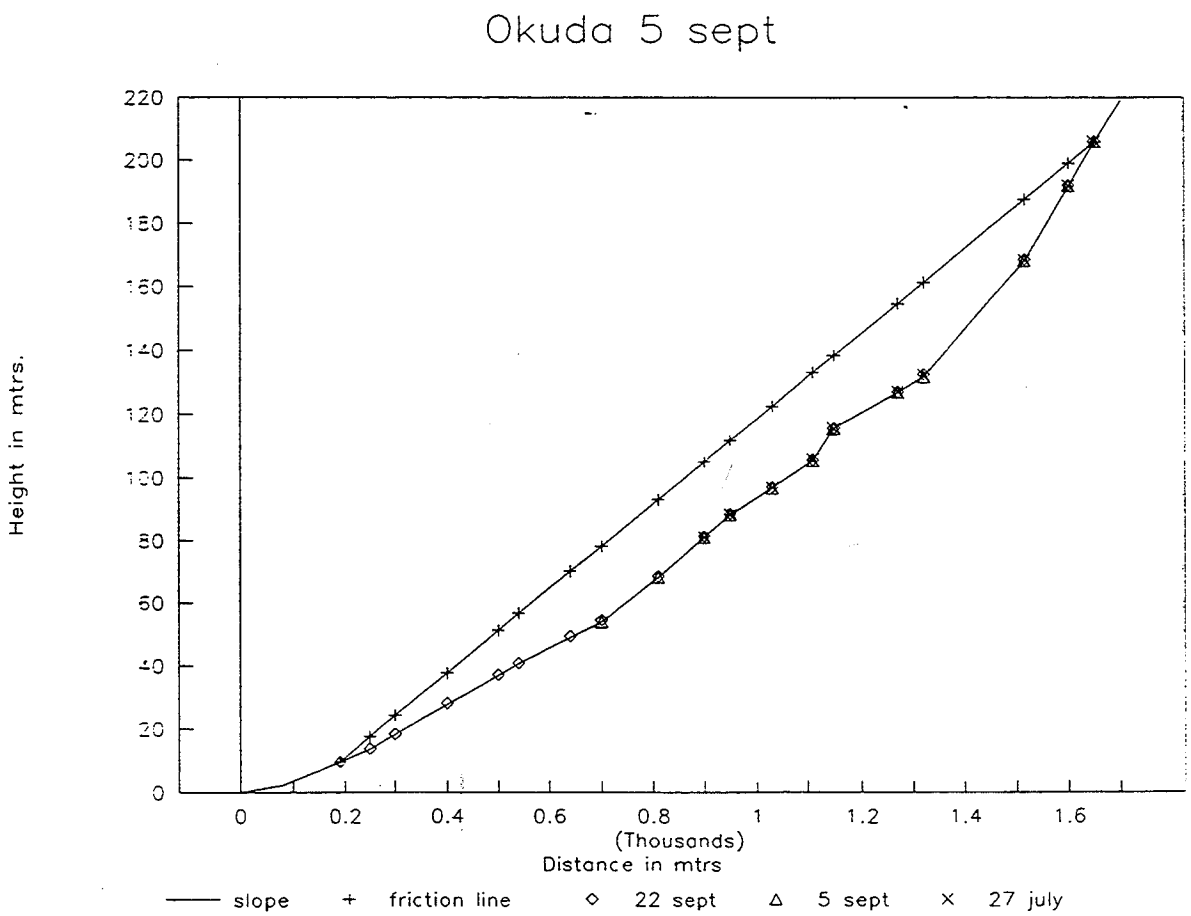

Figure 13: The friction lines of three debris flow runouts (27 july, 5 and 22 sept. 1982) in the Kamikami hori valley Japan. (data obtained from Suwa and Okuda (1985).

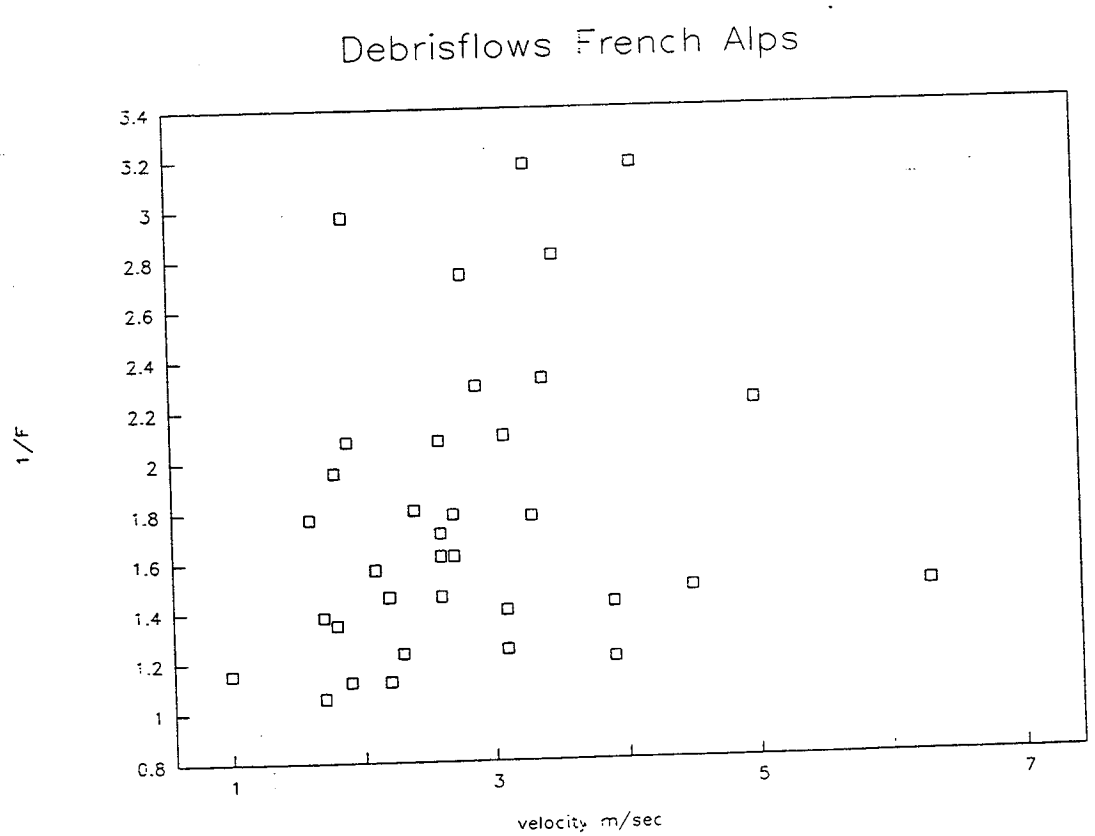

Figure 14: The relation between 1/F and velocity of different debris flows in the French Alps in the Barcelonnette basin.

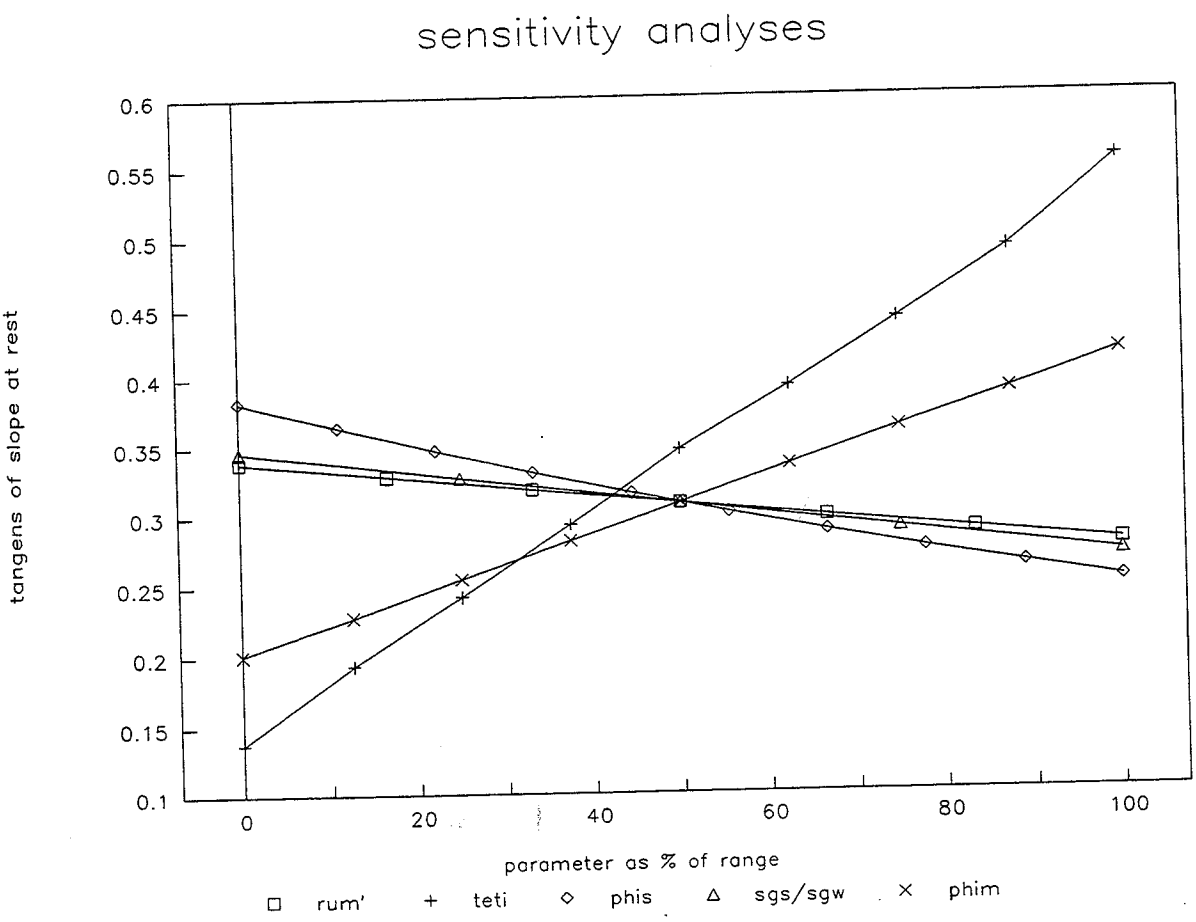

Figure 15: Sensitivity analysis of a run out model for debris flows. The threshold slope for stopping (y-axis) against dynamic pore pressure (rum'), initial slope (teti), static (phis) and dynamic (phim) friction and bulk densities (sgs/sgw).

The second problem in describing the mobility of debris flows is the definition of the strength threshold component τ_0 in equation (34). This component is important for the determination of the run out distance of the debris flow.
The strength threshold component can be considered as:

-an undrained cohesion term including pore pressure conditions,
-a drained friction angle term excluding pore pressure,
-a drained cohesion and friction term.

The models of Johnson (1970) work with an undrained cohesion term. In this case the debris flow will stop at a certain threshold slope angle or at a critical minimum thickness of the flow.
If a drained friction angle is assumed the strength τ_0 is built up of a mobile friction angle of the material and a pore pressure term obeying the Coulomb law: $\tau_0 = (\tau - u)\tan\varphi_m$ where τ is the total normal stress, u is the pore pressure during movement and φ_m the mobile friction angle of the material. In this concept of a drained φ-strength material the stop of the debris flow is only dependent on a threshold slope angle which depends on the mobile friction angle of the material and the existing pore pressure. The problem is to determine the existing mobile friction angle and the pore pressure during moving which may be higher than static pore pressure. A lumped undrained cohesion factor, determined by back analyses, might give a solution to avoid this problem. Another problem remains however wether the threshold conditions for stopping of the debris flow are different for an undrained cohesive material (slope angle and thickness) and a drained φ-material (only slope angle).
The assumption that the debris flow material also has a drained cohesion factor seems unlikely for a highly mobile unconsolidated material.

In the run out model developed in the framework of this EPOCH project, it is assumed that the debris flow mass is a typical φ-material which means that the material stops at a certain slope angle, which is determined by the mobile friction of the material and the existing pore pressure. It is further assumed that the initiation occurs by plastic failure due to a rise of pore pressure in the debris mass which comes from a concentration of run off water or direct infiltration in the debris mass. The debris mass has a certain static friction value φ_s and during movement a dynamic friction factor φ_m. These are important parameters to be measured carefully in the field. The volume of water involved in the debris flow at the start depends on the difference between the static friction angle φ_s of the debris mass at rest and the slope angle θ of the debris mass. A higher difference between these values means a higher amount of water to initiate movement and also a higher mobility of the mass as we will see later. The minimum amount of water required for mobilisation can be calculated by the following simple static equilibrium equation:

$$u_s/\sigma = r_{us} = 1 - [\tan\theta_i/\tan\varphi_s] \qquad 35$$

where

u_s = pore water pressure
σ = total normal weight of debris
r_{us} = pore pressure ratio for at rest condition
θ_i = slope angle of debris at initiation
ϕ_s = static friction angle of the debris

Essential factors for the mobility are:
- the reduction of the static friction angle ϕ_s to a mobile friction angle ϕ_m,
- the increase in pore pressure due to velocity of the fluid,
- the loss of water by drainage of the debris during movement.

In the here proposed model it is assumed, based on current observation, that during the movement an increasing part of the debris becomes immobile due to drainage loss of water while a decreasing volume part stays mobile until no volume is left or the mobile part meets an slope angle θ where the pore pressure ratio is not sufficient to overcome friction (see below). It is further assumed that in the mobile part there is no loss of water during movement.
When the debris starts to move, the pore pressure ratio r_{um} increases because of debris movement (Sassa, 1988) especially when there is nearly no vertical drainage.
If one assumes no loss of water in the mobile part the pore water ratio r_{um} stays constant irrespective of the depth of the flow. The pore pressure ratio can be calculated in the following way:
Equation (35) means that we can write for σ:

$$\sigma = \sigma_w + \sigma_d = u_s/r_{us} \qquad \textbf{36}$$

where
σ_w = normal stress of the saturated layer of the debris
σ_d = normal stress of the unsaturated layer above it

The pore pressure u_m during movement is given by:

$$u_m = \sigma_w r_{um}' \qquad \textbf{37}$$

where r_{um}' is the pore pressure ratio of a debris mass which is totally saturated. r_{um}' has to be determined by experiments. It depends on the velocity of the debris. The experiments of Sassa (1988) showed that the pore pressure ratio r_{um}' tends to develop to a constant value with increasing velocity of the flow towards about 0.8 in case the debris mass is fully saturated. This value is reached at a velocity of about 1 m/sec. These excess pore pressures can be maintained during a certain time even when the mass comes to rest. The pore pressure ratio r_{um} for a moving debris mass which is partially saturated is given by:

$$r_{um} = um/(\sigma_w + \sigma_d) = \sigma_w\, r_{um}'/(\sigma_w + \sigma_d) \qquad 38$$

Combination of (36) and (38) results in:

$$r_{um} = r_{um}'\, r_{us}\, \sigma_w/u_s \qquad 39$$

If we assume at initial failure that the groundwater is moving parallel to the slope we can write:

$$\sigma_w/u_s = \gamma_s / \gamma_w \cos\theta_i \qquad 40$$

where
γ_s = Bulk density of wetted mass
γ_w = Bulk density of the pore fluid
θ_i = Slope angle of the debris mass at initial failure

Hence (39) becomes:

$$r_{um} = r_{um}'\, r_{us}\, [\gamma_s / \gamma_w \cos\theta_i] \qquad 41$$

Note that for the calculation of r_{um} the depth of the moving mass at initiation and during movement and the ratio between the depth of the saturated and unsaturated zone is not required if we assume that no water is lost in the mobile part. Note also that if r_{um}' is constant, so not depending on velocity, r_{um} is also constant. Combining (35) and (41) and substituting r_{us} delivers:

$$r_{um} = r_{um}'\, [\gamma_s / \gamma_w \cos\theta_i]\, [1 - \tan\theta_i/\tan\varphi_s] \qquad 42$$

Equation (42) shows that the amount of pore pressure generated in the fluid is among others dependent on the difference in the static friction angle φ_s and the slope angle at the start of movement θ_i.
Along the debris of the flow path the inverse Safety Factor 1/F can be calculated as follows:

$$1/F = \tan\theta / (1 - r_{um}')\, \tan\varphi_m \qquad 43$$

where
θ = the slope angle at a certain place along the debris flow path
φ_m = the mobile friction angle of the debris

In this scenario the amount of water at the start of the debris flows is back calculated according to the principle of limit equilibrium conditions of the debris mass. This is the minimum amount of water required for initiation. However more water than this calculated minimum amount can be supplied to the debris at the start. Sudden waves of water with mud, with heights higher than the critical ground water level, can pass through the debris. The water and mud is delivered through sudden rapid discharges from the catchment above the debris mass. Also extra run off water can be supplied from adjacent slopes along the flow path. These conditions are difficult to model if no hydrological details of the surrounding area are known. In that case it is advised to make a conservative estimate and to assume that the debris mass is completely filled with water and hence:

$$r_{um} = r_{um}' \qquad 44$$

Figure 15 shows a sensitivity analysis for the calculation of the critical angle where the debris flow will stop according to equation (43) for different values of r_{um}' ranging from 0.6-0.75, tan θi from 0.30-0.75, tan ϕ_s from 0.57-0.75, γ_s/γ_w from 1.2-1.6 and tan ϕ_m from 0.3-0.58. The graph shows that the initial slope angle and the mobile friction angle are the most sensitive parameters. Unfortunately the last one is very difficult to measure.

DISCUSSION AND RECOMMENDATIONS FOR FURTHER RESEARCH

The inaccesibility of debris flow source areas in mountainous environments, and the danger caused by the activity of processes like (single particle) rockfall have always obstructed the study of debris flow initiation. Modern techniques like video cameras and automatically monitoring equipment will be important for future investigations in such difficult terrain. Other equipment, that has to be taken into the field by researchers must be portable as far as dimensions and weight are concerned. Besides, energy and water supply can be problematic.
All these problems have resulted in only little being known yet of debris flow source areas, even though debris flows are an important transport mechanism in many mountainous areas. A lot more work remains to be done to improve the knowledge of debris flow source areas and debris flow initiation conditions. This must in part come from direct field measurements and observations of processes at work in and characteristics of debris flow source areas. On the other hand, simple methods have to be found to be able to make statements on debris flow activity and hazard over larger areas.

Some recommendations for further research:
- Video camera recordings of processes in debris flow source areas, especially during high-intensity rainstorms.
- Detailed rainfall data: short-duration intensities and intensity-frequency-duration

curves.
- Monitoring of rainfall and runoff in debris flow source areas.
- Monitoring of runoff sediment content.
- Measurement of flow characteristics of overland flow containing a high amount of sediment.
- Measurement of flow characteristics of sediment-rich fluid through pores of coarse debris.
- Inventarization of debris flow source areas and their characteristics. Characteristics are morphological, lithological, climatological, hydrological and strength parameters.
- Measurement of static and dynamic angles of internal friction for coarse debris.
- Datation of debris flow deposits: relative and absolute.

REFERENCES

BOVIS M.J. & DAGG. B.R. 1987. *Mechanisms of debris supply to steep channels along Howe Sound, southwest British Columbia.* In: Erosion and Sedimentation in the Pacific Rim. (Proceedings of the Corvallis Symposium, august 1987), pp. 191-200. IAHS publications 165.

BOVIS M.J. & DAGG. B.R. 1988. *A model for debris accumulation and mobilization in steep mountain streams.* Hydrological Sciences Journal/Journal des Sciences Hydrologiques, vol. 33, nr. 6, pp. 589-604.

CAINE N. 1980. *The rainfall intensity-duration control of shallow landslides and debris flows.* Geografiska Annaler Series A, vol. 62, pp.23-27.

COSTA J.E. 1984. *Physical geomorphology of debris flows.* In: Costa, J.E. & P.J. Fleisher (eds.): Developments and Applications of Geomorphology, Springer Verlag, Berlin/Heidelberg, 372 pp. (pp.268-317).

DUNIN F.X. 1976. *Infiltration: its simulation for field conditions.* In: Rodda, J.C. (ed.): Facets of Hydrology, Wiley, London, 368 pp. (pp.199-227).

GREEN W.H. & AMP G.A. 1911. *Studies on soil physics. Part I: The flow of water and air through soils.* Journal of Agricultural Sciences, nr. 4, pp. 1-24.

HOVIUS N. 1990. *Ontstaan van puinstromen. Een onderzoek naar de aard van ontstaansgebieden van puinstromen en naar de manier waarop puinstromen ontstaan, in het zuidelijk deel van de Franse Alpen.* Unpublished report Utrecht University, Department of Physical Geography, 122+69 pp. (in dutch).

INNES J.L. 1983. *Debris flows.* Progress in Physical Geography, vol. 7, nr. 4, pp. 469-501.

JOHNSON A.M. 1970. *Rheological properties of debris, ice and lava; debris flow in channels.* In: Johnson, A.M. (ed.): Physical Processes in Geology, Freeman, Cooper & Company, San Francisco, 577 pp. (pp. 495-514).

JOHNSON A.M. & RODINE. J.R. 1984. *Debris flow.* In: Brunsden, D. & D.B. Prior (eds.): Slope Instability, Wiley, London, 620 pp. (pp. 257-361).

OLYPHANT G.A., CARLSON C.P. & HARPER.D. 1991. *Seasonal and storm-related aspects of sediment yield from a rapidly eroding coal refuse deposit in southwestern Indiana.* Water Resources Research: a Journal of the Sciences of Water, vol. 27, nr. 11, pp. 2825-2833.

PHILIPS J.R. 1957. *The theory of infiltration. I. The infiltration equation and its solution.* Soil Science, 83, pp. 345-357.

POSTMA R. 1988. *Model voor de initiatie van debris flows.* Unpublished report Utrecht University, Department of Physical Geography, 20pp.

SASSA K. 1988. *Geotechnical model for the motion of landslides.* In: C. Bonnard, Landslides. Proceedings of the Vth International Symposium on landslides, Lausanne. Balkema, Rotterdam, pp. 37-56.

SMITH R.E. & PARLANGE J.Y. 1978. *A parameter-efficient hydrologic infiltration model.* Water Resources Research: a Journal of the Sciences of Water, vol. 14, nr, pp. 533-538.

SUWA H. & OKUDA S. 1985. *Measurements of debris flows in Japan.* Proceedings of the IVth International Conference and Field Workshop on landslides, Tokyo, pp. 391-399.

TAKAHASHI T. 1978. *Mechanical characteristics of debris flow.* Journal of the Hydraulic Division, Proceedings ASCE, vol. 104, nr. HY8, proc. paper 13971, pp. 1153-1169.

TAKAHASHI T. 1980. *Debris flow on prismatic open channel.* Journal of the Hydraulic Division, Proceedings ASCE, vol. 106, nr. HY3, proc. paper 15245, pp. 381-396.

TAKAHASHI T. 1981. *Debris flow.* Annual Review of Fluid Mechanics, vol. 13, pp. 57-77.

VAN ASCH TH.W.J. & VAN STEIJN. H. 1991. *Temporal patterns of mass movements in the French Alps.* Catena, vol. 18, nr. 5, pp. 515-527.

VAN DEURSEN W.P.A. & KWADIJK. J. 1990. *Using the Watershed tool for modelling the Rhine catchment.* Unpublished report Utrecht University, Department of Physical Geography.

VARNES D.J. 1978. *Slope movement types and processes.* In: Schuster, R.L. & R.J. Krizek (eds.): Landslides, analysis and control. Washington, Transportation Research Board of the National Academy of Sciences, special report nr. 176, pp. 11-33.